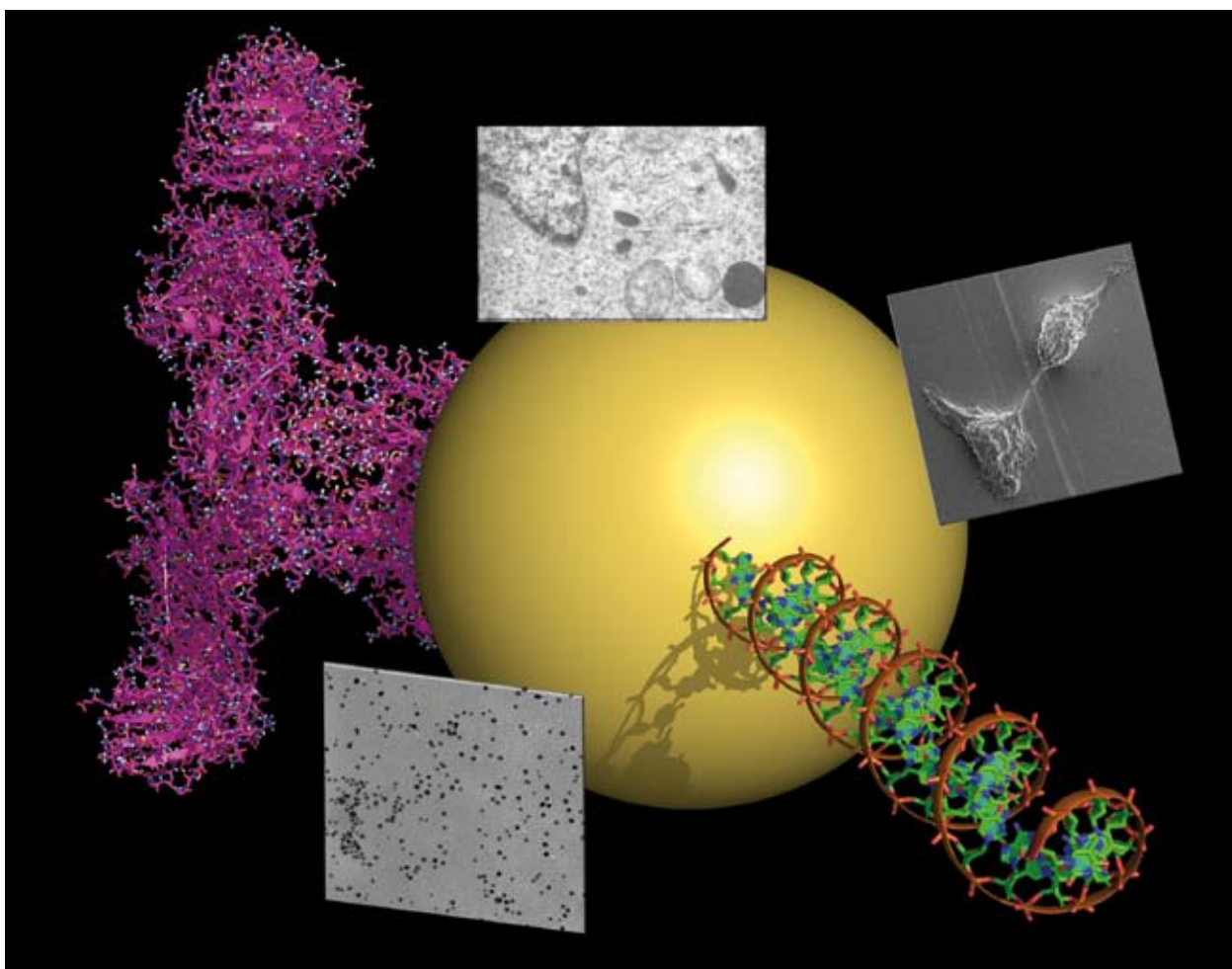


Chem Soc Rev

This article was published as part of the

2008 Gold: Chemistry, Materials and Catalysis Issue

Please take a look at the full [table of contents](#) to access the
other papers in this issue



Shape control in gold nanoparticle synthesis†

Marek Grzelczak,^a Jorge Pérez-Juste,^{*a} Paul Mulvaney^{*b} and Luis M. Liz-Marzán^{*a}

Received 26th May 2008

First published as an Advance Article on the web 7th July 2008

DOI: 10.1039/b711490g

In this *tutorial review*, we summarise recent research into the controlled growth of gold nanoparticles of different morphologies and discuss the various chemical mechanisms that have been proposed to explain anisotropic growth. With the overview and discussion, we intended to select those published procedures that we consider more reliable and promising for synthesis of morphologies of interest. We expect this to be interesting to researchers in the wide variety of fields that can make use of metal nanoparticles.

1. Introduction

A fundamental goal of materials science is the design and synthesis of materials with tailored shape and size. This goal underpins the growing interest in the fabrication of intelligent and complex materials such as artificial bones, teeth and cartilage, nanowires for electronic circuitry, shape memory alloys, and plasmon based sensors. Growing sophistication in colloid based crystal nucleation and synthesis is enabling some of these targets to be realised. In particular, there has been tremendous progress over the past decade in the synthesis of gold and silver nanocrystals of various sizes and shapes and with good yield and monodispersity.^{1–5} The mechanisms underpinning these synthetic methods have evolved empirically and there is no accepted mechanism to explain how shape control works, particularly in a material such as gold where the surface free energies and chemistry of the major facets are similar. It is perhaps salient to point out that gold nanoparticles have been synthesised for over 2000 years in a

whole range of media including glasses, salt matrices, polymers, the gas phase and in water—invariably these methods have resulted in the formation of spheres. It is only in the past decade that significant progress towards non-spherical nanoparticle synthesis has been achieved. In this tutorial review we summarise some of the emerging protocols for shape control of gold nanocrystals, and we examine some of the mechanisms currently proposed to help explain this important advance in materials science. Lofton and Sigmund provided the first such review in 2005,⁶ focusing on the crystallographic aspects of shape control, including twinning. Here the focus is on how different chemical environments appear to promote the growth of different shapes, from platonic solids through to rods and branched metal nanocrystals.

2. Anisotropic gold nanoparticles in water

The first point to make about the vast majority of reported syntheses of shape controlled gold nanoparticles is that they rely on seed-mediated growth. Indeed it is important to recognise that the conditions necessary for nucleation of nanocrystals are exactly the opposite to those required for selective growth of facets. Small seed particles of gold are generated under conditions of high chemical supersaturation. This leads to the fastest nucleation rate and almost invariably

^a Departamento de Química Física and Unidad Asociada CSIC, Universidade de Vigo, 36310 Vigo, Spain. E-mail: juste@uvigo.es. E-mail: lmarzan@uvigo.es; Fax: +34 9868 12556; Tel: +34 9868 12298

† Part of a thematic issue covering the topic of gold: chemistry, materials and catalysis.

Marek Grzelczak received his MSc degree in chemistry in 2004 from the Adam Mickiewicz University (Poland) and his PhD from the University of Vigo (Spain) in May 2008. He spent part of his PhD at the University of Duisburg-Essen (Germany) and Aristotle University of Thessaloniki (Greece). His current research interests focus on the synthesis and characterisation of anisotropic, multifunctional nanostructures.

Jorge Pérez-Juste obtained his chemistry degree from the University of Santiago de Compostela in 1995, and his PhD degree in chemistry from the University of Vigo in 1999. He worked as a postdoctoral fellow at UCSC in 2000 and at Melbourne University (Australia) in 2002 and 2003. He is currently a Ramón y Cajal research fellow at the University of Vigo.

Paul Mulvaney is currently an ARC Federation Fellow and Professor of Chemistry at the University of Melbourne. After a PhD from the University of Melbourne (1989), he was a research scientist at the Hahn-Meitner Institute, Berlin (1989–1992), and later a Humboldt Research Fellow at the Max-Planck and CAE-SAR Institutes. His interests include surface plasmon spectroscopy and nanoscale chemistry and physics.

Luis M. Liz-Marzán received his PhD from the University of Santiago de Compostela in 1992. He then moved to Utrecht University as a post-doctoral research associate. He joined the University of Vigo in 1995, where he currently is a full professor. His current interests include nanoparticle synthesis, colloidal composites, nanoplasmonics, and the use of metal nanoparticles as biosensors.

to spherical nuclei with sizes between 1 and 5 nm. Such conditions ensure rapid growth of all crystal surfaces but are contraindicated for shape control. As a consequence, shape control is commonly achieved through a two-step process, termed “seed-mediated growth”. In the first step, very small, reasonably uniform, spherical seed particles are generated. The reaction conditions are then altered and more gold ions and a different reductant are added, together with some form of shape templating surfactant or molecule, and the seeds are grown into larger particles of particular morphologies or habits. Typically the growth stage is much slower and proceeds under milder reducing conditions than the nucleation stage.

Nanorods

The growth of gold nanorods is, within the field of anisotropic nanoparticle synthesis, the most established protocol, in terms of the degree of control of the size, shape and monodispersity. Of the reported procedures for gold rod formation, seed-mediated growth has been by far the most efficient and popular approach. The original idea was that cationic surfactant micelles could serve as a “soft template” for directing nanoparticle growth and could additionally provide colloidal stability for the synthesised nanoparticles.⁷ However, the role played by the seed particles is also critical. Furthermore, the presence of small amounts of silver nitrate during the synthesis has a dramatic effect on the final shape and crystalline structure of the particles.⁸ Consequently, in the next section we review the seeded-growth based synthesis of gold rods, with special emphasis on the crystalline structure of the seeds and the use of silver nitrate during growth.

Citrate-capped gold nanoparticles, prepared through reduction of HAuCl_4 with borohydride ions have traditionally been chosen as seeds for gold nanorod growth. An important issue has been the origins of the twinning planes observed in such rods. It was originally suggested that freshly made seeds are single crystals, which become multiply-twinned particles (MTPs) upon addition of the growth solution.⁹ However, detailed TEM analysis revealed that the gold seeds are intrinsic MTPs, with diameters of 4–5 nm. An important piece of work in this respect was carried out by Liu and Guyot-Sionnest,¹⁰ who observed differences between the crystalline structures of citrate and cetyl trimethylammonium bromide (CTAB) stabilised seeds (See Fig. 1d, e), confirming the multiply-twinned structure of citrate-capped seeds. This kind of structure is generally recognised as decahedral, where the twinned crystals display five-twin boundaries, with all crystal faces formed by $\{111\}$ planes.

This method was first reported by Murphy’s group.¹¹ In a typical synthesis, ascorbic acid, a mild reducing agent, is added to an aqueous CTAB solution of HAuCl_4 to selectively reduce Au(III) to Au(I) , followed by addition of the seed solution (containing citrate-capped, penta-twinned gold nanoparticles), which catalyse reduction of Au(I) ions on their surface. Careful choice of the experimental conditions allows the growth of the seeds into nanorods. By means of a multi-step seeding process, nanorods with aspect ratios ranging from 4.6 up to 18 can be obtained, although in rather low yields (up to 4%). Pérez-Juste

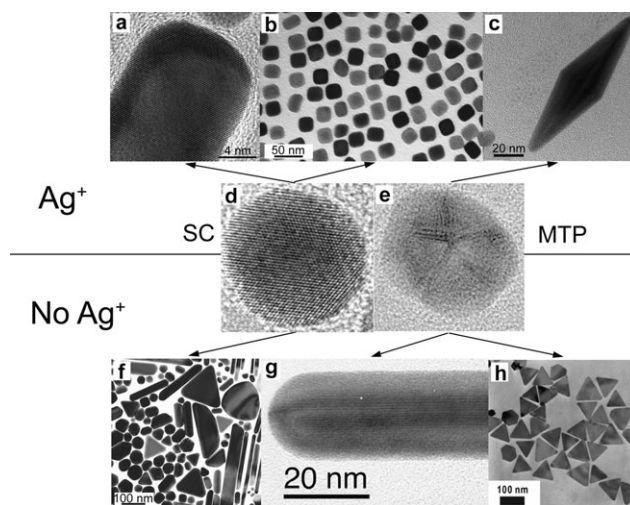


Fig. 1 Morphology dependence of gold nanoparticles grown from either single crystal (d) or multiply twinned (e) seeds, in the presence (a–c) and absence (f–h) of silver nitrate. Figures c and h reproduced with permission from ref. 10 and 18, respectively.

*et al.*¹² subsequently demonstrated that when the temperature and CTAB concentrations are reduced, nanorods with shorter aspect ratios (1 to 6) can be obtained, with yields up to 50%. The aspect ratio could be precisely controlled through a careful variation of the amount of seed added to the growth solution; it was observed that a decrease in the reaction rate favours nanorod formation over isotropic growth, thereby increasing the yield of nanorods. These authors also observed that the aspect ratio increases monotonously throughout the growth process, which is not observed when Ag^+ is present during reduction.⁴ Interestingly, the rods prepared in this way (MTP seeds, no Ag^+) exhibited a pentagonal cross section and perfect five-fold twinning (Fig. 1g).

Addition of silver nitrate during Au nanorod growth from penta-twinned seeds leads to an increase in the gold nanorod yield and greatly improves control over the aspect ratio. A similar effect had been previously reported for the electrochemical synthesis of gold nanorods, where immersion of a silver plate in the electrolytic solution was required to control the aspect ratio of the obtained particles.¹³ In an early work, Murphy and co-workers⁷ explored the influence of adding either silver nitrate or cyclohexane to the growth solution, and found that this resulted in the formation of up to 50% needle-like particles (latter recognised to be bipyramids, see Fig. 1c). Following up on this work, Liu and Guyot-Sionnest were able to synthesise monodisperse bipyramids with a yield of around 30% and aspect ratios up to 5.¹⁰

Contrary to the results obtained with citrate-capped Au nanoparticle seeds, when CTAB is used during borohydride reduction of HAuCl_4 , single crystalline seeds are obtained, which are also smaller in size. CTAB-capped Au seeds were first used (in the presence of AgNO_3) by Nikoobakht and El-Sayed,⁸ who obtained single crystalline Au nanorods in unprecedented high yields. However, only after the HRTEM study by Liu and Guyot-Sionnest,¹⁰ was it understood that the seeds were single crystals with diameters around 1.5 nm (Fig. 1d). Because of the extremely high yield of nanorods

obtained from single-crystal seeds, this has become by far the most popular synthetic route. This work also demonstrated that a twin plane is not a pre-requisite for rod growth.

One important piece of evidence for the valuable role played by AgNO_3 as an additive is that, even when using single crystalline seeds, growth in the absence of silver ions leads to nanoparticles with a wide variety of shapes including spheres, triangles, and rods. Fig. 1f shows a representative TEM image of the obtained nanoparticles. It is evident that there is no control over the particle shape and morphology.

Conversely, by using CTAB-capped, rather than citrate-capped seeds, and adding AgNO_3 , a spectacular yield of gold nanorods of ca. 99% can be obtained routinely, with aspect ratios ranging from 1.5 up to 5, simply by varying the amount of AgNO_3 added. The aspect ratio of the nanorods can also be controlled consistently by keeping the silver nitrate concentration constant and varying the amount of seed.⁴ An important contribution towards understanding the role of both Ag^+ ions and the crystalline structure of the seeds was again provided by Liu and Guyot-Sionnest,¹⁰ who found that by controlling the pH of the reaction between 2 and 4, the reaction time is increased (from 1 h up to 2 h) and longer nanorods can be obtained.

Platonic nanoparticles

Five platonic solids can be constructed by selecting a regular polygon and having the same number of such polygons meeting at each corner: tetrahedra (3 triangles), hexahedra (4 squares), octahedra (four triangles), icosahedra (5 triangles) and dodecahedra (3 pentagons). All aqueous based synthetic protocols reported to date for making such platonic nanocrystals from gold are based on the growth of smaller seeds. However, formation of a specific shape is usually restricted to a specific choice of the reaction parameters. For example, Sau *et al.*¹⁴ showed that either hexahedra (cubes) or octahedra can be obtained through variations of the silver nitrate mediated synthesis of gold nanorods on single crystal seeds.⁸ For example, while cubic particles (Fig. 1b) can be obtained in 85% yield at low CTAB and high ascorbic acid concentrations, octahedra (80% yield) are obtained at comparatively high CTAB and low ascorbic acid concentrations, albeit with truncated {100} and {111} faces. Low CTAB concentrations apparently favour faster deposition of Au atoms onto the {111} facets of the seeds, until they disappear, giving rise to {100} facets exclusively. Truncated octahedra can be also obtained using single crystalline gold nanorods as seeds. For example, Wang and co-workers¹⁵ recently reported preferential transverse overgrowth on Au nanorods in the presence of glutathione or cysteine, with complete suppression of growth along the longitudinal axis. During this process, gold nanorods underwent several, stepwise, morphological changes, becoming first peanuts, then truncated octahedra and finally evolving into faceted spheres.

Nanoplates

Other types of anisotropic nanoparticles include triangular or hexagonal plates. The main interest in these particles is due to their sharp edges, which lead to high local electric field gradients under illumination, making them attractive

candidates for a number of applications such as optical biosensing and surface-enhanced Raman spectroscopy (SERS). The seed-mediated growth of gold nanoplates is frequently observed during variations to the synthesis employed for gold nanorods. Some changes in the synthetic procedure such as an increase in the pH or surfactant concentration, or the addition of extra halide ions can lead to the formation of planar nanostructures. Unfortunately, all current procedures still result in rather low yields (40–65%) compared to those for the one-dimensional structures (ca. 95–99% for gold nanorods) and a purification step is needed in order to eliminate isotropic structures.

Trigonal prisms were synthesised by Mirkin *et al.*¹⁶ using a procedure that was fairly close to that reported by Murphy *et al.* for long gold rods (with no silver nitrate).¹⁷ Citrate-capped seeds were grown in three stages, in a saturated CTAB solution containing gold salt, ascorbic acid and NaOH. Nanoprisms were obtained with average edge-lengths and thicknesses of 144 and 8 nm, respectively, and yields up to 65%. Larger prisms, with edge lengths up to 220 nm were also grown using smaller prisms as seeds.

Other useful variations to the seed-mediated method include the addition of salts or polymers to the growth solution. Addition of KI at pH 4 increases the yield of gold nanoprisms up to 45% (Fig. 1h).¹⁸ Based on a series of control experiments the authors proposed a possible growth mechanism for nanoprisms involving growth inhibition of the {111} facets by strongly bonded halide ions (see growth mechanism section). Alternatively, Yun and colleagues found that using poly(vinyl pyrrolidone) (PVP) instead of CTAB¹⁹ and sodium citrate as reducing agent yields single crystal nanoplates with lateral dimensions between 80 and 500 nm and thicknesses of 10–40 nm, depending on the molar ratio of PVP to HAuCl_4 .

Several natural reducing agents have also been demonstrated to induce formation of non-spherical morphologies. One of the most prominent examples of biologically prepared gold nanoparticles is gold trigonal nanoplates grown in the extract of living plants, extensively reported by Sastry's group. For example, gold nanoplates were obtained in a 50% yield by using a boiled extract of lemongrass leaves as both reducing and shape directing agent.²⁰ The authors claimed that sugars (aldoses) and aldehydes/ketones are the main compounds responsible for nanoparticle formation. The average edge length of the prisms was observed to vary from 100 to 1800 nm by varying the concentration of lemongrass extract in solution.²¹

In another approach,²² Lee *et al.* demonstrated the synthesis of planar gold nanostructures in yields up to 80%, with side lengths in the range 0.6–3 μm and 19 nm thickness, using bovine serum albumin (BSA) as the reductant and stabiliser. Interestingly, they found that introducing Ag^+ ions into the growth solution altered the kinetics of Au(III) reduction, allowing the lateral size of the Au nanoplates to be varied over a very large size range, from a few microns down to just a few tens of nanometres.

Branched nanostructures

Another important group of gold nanostructures are “branched” particles. Although these are obviously more complex structures and correspondingly more difficult to

synthesise reproducibly, they generate interest because of their sharp edges and the correspondingly high localisation of any surface plasmon modes. This makes them potential candidates for a number of applications, including SERS based detection and analysis, as is also the case for nanoplates. However, there are substantial difficulties in forming gold nanostructures of complicated morphologies in homogeneous aqueous solution because noble metal crystals usually exhibit a highly symmetric, face-centred cubic (fcc) structure and the dominant facets possess similar surface free energies for the major facets. Again the seed-mediated method is one of the most useful for the preparation of branched structures. The presence of surfactants, the type of reducing agent and the presence or absence of silver ions, are all key factors in the syntheses. For example, Sau *et al.*¹⁴ proposed the synthesis of branched nanoparticles by varying the seed to gold salt ratio and the amount of reducing agent in order to increase the rate of gold ion reduction and thereby induce branching. On the other hand, Chen *et al.*²³ demonstrated the use of Ag triangular platelets as seeds for the synthesis of branched Au nanoparticles (monopods, bipods, tripods and tetrapods, with yields of up to 60%) by reduction of gold ions with ascorbic acid in alkaline CTAB solution; however, the structure of the seeds did not seem to be related to the final particle morphology, since similar branched particles were obtained when using other types of seeds (albeit with lower yields). While various arguments have been used to explain branching, it is still too early to really understand what provides the selective driving force for this growth mode.

3. Growth mechanisms

In the previous section, we summarised some of the key advances in the synthesis of gold nanoparticles with different morphologies. In this section we turn our attention to the different growth mechanisms that have been proposed to explain the formation of anisotropic gold nanoparticles in water.

Growth mechanisms for gold nanorods in the absence of silver ions

The penta-twinned structure of nanorods grown in the absence of silver nitrate was proposed by Lofton and Sigmund⁶ as the origin of anisotropic growth. In this process, MTP seeds would stretch, providing the necessary symmetry breaking, so that rods would form because of the increased strain formed in the lattice as an atom is located further away from the central axis. This strain originates from the fact that there is incomplete filling of space when five tetrahedra (tetrahedral angle = 70.53°) are placed next to each other. In order to fill the space, the lattice is strained—a phenomenon which has in fact been directly measured.²⁴ Thus, in the model proposed by Lofton and Sigmund, the more strained facets are inhibited, causing the decahedra to elongate in the unstrained direction not increasing the strain, parallel to the twin planes. This could explain the break in growth symmetry but does not explain further growth in one direction of the rods once they have formed.

The opposite criticism can be applied to the electric field model proposed by Mulvaney and co-workers,¹² This model is based on the mechanism commonly postulated to explain

dendritic growth on electrodes. It attributes the growth of rods to a higher rate of mass transfer of gold ions to the tips due to the asymmetric double layer around the rod. According to the authors the CTAB plays two key roles. First, the gold rods are positively charged due to the presence of a bilayer of the cationic surfactant. Second, the Au(I) ions (originating from reduction of Au(III) by ascorbic acid) are also bound to CTAB micelles in the solution. Thus, the rate of growth of the gold seeds in the presence of CTAB is controlled by the flux of gold-laden, cationic micelles to the CTAB-capped gold particles. Since both the rods and the micelles possess very high zeta potentials (+90 mV), the rate of transfer of the Au(I) ions to the rods should be drastically retarded. Indeed, it is observed that gold seeds grow almost 1000 times more slowly in the presence of CTAB. The surface potential due to the surfactant decays more quickly at the tips due to the higher curvature and consequently the micelles' flux is higher at the tips. Calculations of the diffusion-migration rate of the micelles to the rods within the double layer confirm that the encounter rate will be much higher at the tips. Preferential tip-oxidation of nanorods also has been reported, which strongly supports the electric field-directed interaction between the nanoparticles and CTAB micelles. While this mechanism can explain why the rod tips grow faster than the lateral facets, it does not explain the initial symmetry-breaking needed to avoid spherical growth.

Murphy and co-workers proposed that steric and chemical factors could play an important role in determining the preferential interactions between the cationic quaternary ammonium head groups from CTAB and the growth sites on the lateral edges and faces of gold nanorods.²⁵ They raised the possibility that surfactant-containing complexes such [AuBrCTA] are specifically incorporated into the {100} side edges, whereas non-complexed ion-pairs or Au(0) atoms/clusters are added to the {111} end faces. The discrimination between sites could be due to the increased stability of the close-packed {111} surfaces compared to the edge sites, which would contain numerous defects. Moreover, the large [RNMe₃]⁺ headgroup of CTAB (diameter = 0.814 nm, area = 0.521 nm²) and the long alkyl chain are more readily accommodated on the {100} side edges, than on close-packed {111} faces, where the Au–Au spacing is too small to facilitate epitaxy. As the nanorods grow in length, the area of the side faces increases, and this could facilitate the assembly of a bilayer of CTAB molecules at the crystal surface. The first monolayer binds with the headgroup pointed down towards the surface and adsorption in this orientation is driven by the presence of chemisorbed bromide ions. The exposure of the alkyl chains to the solvent is energetically unfavourable and would result in the adsorption of a second surfactant layer, with the CTAB's headgroups facing the solvent. In turn, the bilayer would provide additional stabilisation and growth inhibition, and this could explain why elongation of the nanorods is rapid once the shape anisotropy has been established, in a “zipping” type of mechanism.

Growth mechanisms for gold nanorods in the presence of silver ions

To understand the role of silver nitrate on the growth of gold nanorods it is necessary to focus on the possible reaction

products of silver nitrate and the growth solution containing CTAB, gold salts and ascorbic acid. The addition of AgNO_3 to CTAB in aqueous solutions leads to immediate formation of AgBr and, consequently, AgBr is predicted to play an important role in the mechanism. It has been hypothesised that Ag^+ ions adsorb onto the Au particle surface in the form of AgBr and that this restricts growth. Murphy and co-workers⁷ observed that, after adding silver nitrate to the growth solution, the characteristic silver surface plasmon band at 400 nm could not be observed, but when the pH of the solution was increased, silver nanoparticle formation was observed. This seems to suggest that silver ions are not reduced to the metal during rod growth.

Liu and Guyot-Sionnest¹⁰ proposed a more elaborate explanation for the role of the Ag^+ . They suggested that underpotential deposition of metallic silver occurs on the different crystal facets of gold, leading to symmetry-breaking and rod formation. Since this is an interesting concept that can result in more general application, we outline below the basic features of underpotential deposition.

Underpotential deposition²⁶ is an important process that occurs during metal adlayer formation onto a metallic substrate. It is widely observed that, when a metal working electrode is slowly cathodically polarised, ions of a second, less noble metal can be deposited onto the substrate forming a film. Critically, it is frequently observed that there is an initial deposition of a metal monolayer at potentials much more positive than the Nernst potential of the metal being deposited. This deposition of a first and sometimes second monolayer is called underpotential deposition (UPD). It comes about because the adsorbed metal atoms form a bond to the substrate stronger than the bond between the adatoms themselves. The first layer of metal adatoms is therefore more noble than the subsequent layers, causing the initial monolayer of adatoms to form a complete monolayer rather than islands or clusters on the surface. The “wetting” of the surface is driven by the lower free energy for the system if each adatom binds to the substrate. Thereafter deposition occurs at the bulk Nernst potential and this signals that the adsorbed metal layers exhibit the electrochemical properties of the bulk metal. In Fig. 2, we show the important correlation made by Gerischer and co-workers who proved that the strength of the UPD effect is directly correlated to the difference in work functions of the substrate and adsorbate.^{27,28} The UPD effect has been used to great advantage in synthesising core-shell metal colloids. Under reducing conditions, electrons are transferred to the seed metal nanoparticles, polarising them cathodically. These reductants can simply be added to the metal colloid or they may be generated *in situ* photolytically or radiolytically, to ensure homogeneous reducing conditions.²⁹ The deposition of the metal layers then occurs homogeneously for at least the first two monolayers if the UPD conditions are fulfilled, *i.e.* the work function of the seed particle metal is higher than that of the shell metal. Systematic work on this approach to the formation of core-shell metal particles was carried out in Henglein’s group at the Hahn-Meitner Institute in the early 1990s. By combining electron microscopy with surface plasmon spectroscopy of the particles during electrodeposition, processes such as chemisorption, cathodic polarisation, metal

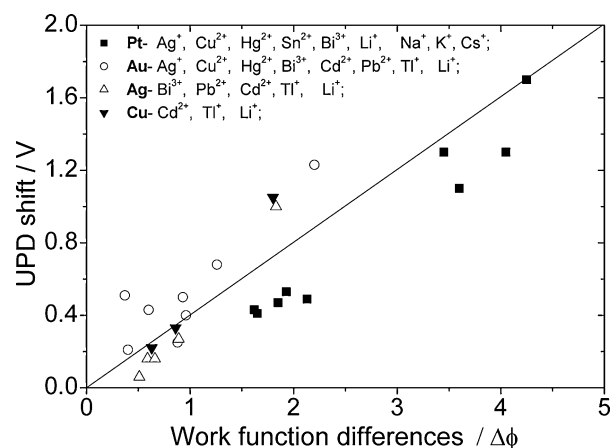


Fig. 2 UPD shift for metal deposition vs. the difference in work functions of the two metals.

adatom deposition, alloying and corrosion resistance could be studied on metal colloids for the first time. The deposition of Pb, In, Tl, Cd, Cu and Sn onto Ag and Au colloids as well as the poisoning reaction of colloidal Pt by lead ions were investigated.²⁹ The importance of UPD is highlighted by two key observations. Firstly, Cu could not be deposited homogeneously onto silver particles, which is consistent with the observations of Gerischer for electrochemical deposition.²⁷ Secondly, it was also observed that while the base metal shells deposited under reducing conditions were readily dissolved on exposure to air, the first and sometimes second monolayers were not dissolved and remained chemisorbed to the particle surface. It is also worth mentioning that UPD has been used to investigate the crystalline structure of gold nanoparticles. Herrero *et al.*³⁰ studied the Pb UPD process on Au nanorods and demonstrated the presence of {100} ordered domains on the surface of single crystal nanorods, in agreement with earlier HRTEM and electron diffraction studies.⁹

Much of the recent work on UPD has been carried out by STM and AFM and has been restricted almost entirely to the Au {111} surface. Furthermore, to date, very little STM work has been carried out on Ag UPD at Au {111} surfaces in the presence of anions because of the insolubility of silver halides. Nevertheless, Laibinis and colleagues have demonstrated that Ag UPD does occur on Au {111} and that the UPD process is affected by the presence of chloride ions.³¹ They found that the Ag adlayer shifts from a (3×3) layer to a more open structure in the presence of chloride ions, and that there is stoichiometric deposition of Cl^- as a superadsorbed layer during UPD, so that the surface is formally almost a AgCl monolayer. The UPD shift becomes stronger in the presence of Cl^- by some 100 mV, with UPD occurring at almost 500 mV positive of the Nernst potential. Gewirth and co-workers found the UPD shift for silver deposition from silver sulfate to be as much as 900 mV.³² One may conclude from this that even under weak reducing conditions, silver deposition to form an $\text{Ag}(\text{Cl})$ layer is extremely likely and in fact is thermodynamically favoured over reduction of the $\text{Au}(\text{I})\text{-CTA}$ complex.

Whether the silver ions are reduced during growth is surprisingly still unresolved. Elemental analysis by EDAX and EELS does not reveal any silver metal in the final gold

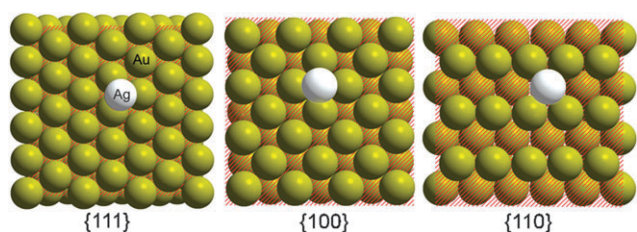


Fig. 3 Schematic illustration of underpotential deposition of silver atoms (light grey circles) on different Au facets. On Au {111} facets, each silver atom has three nearest neighbours, four on {100} facets, and five (one in the second layer right beneath the Ag atom) on the {110} facets. The first and second layers are separated by a dashed plane.

rods, but ICP-mass spectroscopy analysis revealed the presence of Ag up to a total percentage of 4.5%.³³ It is observed that Ag(I) in an aqueous CTAB solution can be reduced to its elemental form by ascorbic acid only above pH = 8,⁷ while in a typical synthesis of gold rods, the pH of the growth solution is about 3. Therefore, silver ions should not be reduced to form silver metal in the bulk, but could still be deposited on the gold surface *via* UPD. It has been concluded that the UPD shift of silver on gold surfaces decreases in the order {110} > {100} > {111}. Fig. 3 shows three different fcc Au metallic facets, the close-packed {111} surface and higher energy {100} and {110} surfaces. Note that silver atoms deposited on the {110} facet have five neighbouring gold atoms, while on the {111} and {100} surfaces, adsorbed silver atoms have just 3 and 4 neighbours, respectively. This is consistent with the UPD data and suggests that the higher the coordination number for the adatom, the higher the UPD shift, and the more noble is the deposited metal monolayer.

Based on these observations, there are several ways that silver might influence rod formation. One model for the role of silver is that the silver monolayer on the Au {110} surface acts as a strong binding agent, inhibiting further growth. Thus the total growth rate of gold on {110} facets may be significantly slowed down. One may hypothesise that the gold nanorod tips, comprised of {100} facets, are only partially covered by silver, and therefore grow faster, which leads to one-dimensional growth along the [100] direction. The growth rate ratio between Au {100} and Au {110} is adjustable by varying the Ag⁺ concentration, which explains the fact that the aspect ratio is controlled by Ag⁺ concentration.

Underpotential deposition can also explain the symmetry breaking needed to initiate rod formation. For example, one may hypothesise that slower growth of {110} side faces and faster growth of {100} end facets lead to breaking of the growth symmetry and this in turn controls the final anisotropic shape of the nanoparticles. However, as with many other models, this does not explain the crucial fact that the single crystalline rods grow along the [100] direction, and yet the {100} facets on the edges of the rods do not grow. Ultimately, it may be that UPD of silver occurs on most of the facets, but poorer coverage of the tips prevents efficient inhibition of the particle growth in that direction.

As has been pointed out in previous sections, AgNO₃ assisted syntheses of gold nanorods on the citrate-capped

and CTAB-capped seeds lead to morphologically different products. The factors affecting the growth mechanism were investigated by Liu and Guyot-Sionnest,¹⁰ who used both CTAB-stabilised seeds (single crystals, diameter 1.5 nm) and citrate-stabilised seeds (MTPs, diameter 3–5 nm) for rod growth in the presence of silver nitrate. The products of growth from CTAB-capped seeds were single crystalline nanorods with different aspect ratios depending on the concentration of AgNO₃, as previously reported. However, growth from citrate-capped seeds led to bipyramidal nanoparticles. What is not clear is whether AgBr or Ag adatoms are the active catalyst driving monocrystalline rod formation.

Liu and Guyot-Sionnest explained the growth mechanism of bipyramids in a similar fashion. These are grown from twinned seeds in the presence of Ag(I). Faster growth along the twinning axis leads to formation of steps, which are blocked by Ag UPD, finally leading to a sharp, bipyramidal structure.

Silver halide mechanism and growth of planar structures

Characterisation of the crystal structure is mandatory for a better understanding of the growth mechanism. It is well known that the main facets exhibited by the sides of gold nanoprisms are {111}-type facets, and detailed examination of the electron diffraction patterns displayed by the prisms indicates twinning in the [111] direction, perpendicular to the main facets of the nanoprism. This twinning produces convex and concave side crystal facets (see Fig. 4), which have different stabilities, and which could provide the driving force for 2D growth. Other driving forces have been postulated based on the differences in surface energies of the growing

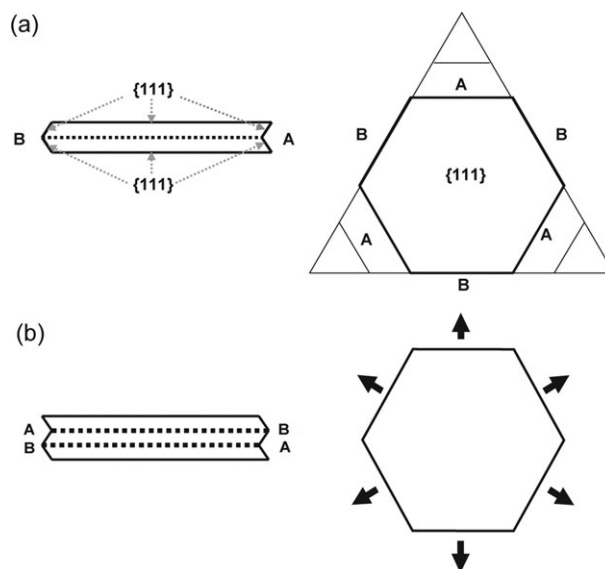


Fig. 4 Silver halide model for a single twin plane and two parallel twin planes. (a) Alternating sides contain convex (A) and concave (B) type facets. The re-entrant grooves of the concave type faces cause rapid growth that is arrested when the face grows itself out, leaving a triangular prism with slow growing convex type facets. (b) The second twin plane causes all six sides to contain concave faces with re-entrant grooves allowing for rapid growth in two dimensions. Reproduced with permission from ref. 6.

crystal. This mechanism, known as the *silver halide model*, was originally applied to silver and gold halide structures, and was investigated in detail by Lofton and Sigmund.⁶ They suggested that the silver halide model can be applied to fcc structures of gold and silver by considering the formation of twin planes on {111}-type faces, where the stacking fault energy is lower than in most metals, decreasing the energy required to form a twin plane. At the six surfaces where the twin plane terminates, the stacking fault of the twin plane causes {111} faces to form in alternating concave or convex orientations (Fig. 4a). On the convex side, an adatom attached to a surface has limited stabilisation energy due to the presence of only three nearest neighbours, so that it can be re-dissolved, thus slowing down the effective growth rate of this surface. On the concave side, where re-entrant grooves are created that increase the number of nearest neighbours for an adatom, the stabilisation energy is increased and growth can be faster than on the convex side. This growth ratio causes the concave side to disappear, leaving a triangular prism. This model can explain not only the growth of trigonal prisms but also the evolution of a hexagonal plane structure, if one additionally assumes the presence of a second twin plane rotated 60° relative to the first twin plane. (Fig. 4b) The second twin plane leads to the presence of concave facets (re-entrant grooves) on all six sides. This leads to the regeneration of adjacent faces to it, allowing for fast growth in two dimensions.

The “iodide-induced mechanism” of Ha *et al.*¹⁸ for nanoprism formation also deserves mention. The most important factor for plane nanoparticle formation was claimed to be the presence of I⁻ in the solution. Based on a series of control experiments, the authors proposed a possible mechanism, involving inhibition of {111} facets by strongly bonded halide ions, which increases in the order Cl < Br < I.

As shown in Fig. 5, in the presence of iodide, a stable CTAB bilayer on an iodide adlayer would form preferentially. However, at the edges of the nanoprisms (Au {110} faces), micelles with higher curvature should be formed, expediting the influx of the chemicals in the edge directions. Associated with this differential reactivity of the Au {110} facet, the crystal growth rate in that direction seems to be more facilitated. This model is somehow related to the electric field mechanism for rod

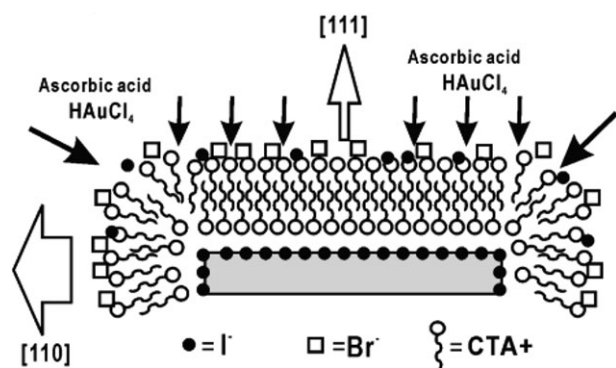


Fig. 5 Schematic cartoon describing the influence of the CTAB template, in conjunction with an iodide adlayer as a passive barrier for crystal growth during the formation of nanoprisms. The white arrows indicate the rate of growth on specific facets. Reproduced with permission from ref. 18.

growth,¹² but comparison with the silver halide model cannot be made directly, since the authors did not clarify whether their nanoprisms also had twin planes on the lateral facets.

4. Anisotropic gold nanoparticles in other solvents

While anisotropic growth of other materials, such as II–VI semiconductors, in organic, non-polar solvents is reasonably well understood, strategies for shape control of gold nanocrystals grown in non-polar solvents have not been forthcoming. To date, all the relevant synthetic methods for non-aqueous shape controlled gold particle synthesis stem from the so-called “polyol process”. This process involves the thermal reduction of a gold salt in an organic solvent with a relatively high boiling point such as poly(ethylene glycol) or *N,N*-dimethylformamide (DMF), in the presence of a polymeric stabiliser, usually poly(vinyl pyrrolidone). Although quite a few variations of this process exist, we restrict this section to discussion of a few key advances in the development of synthetic methods.

Yang and co-workers were the first to propose a unified methodology for the preparation of gold particles (100 to 300 nm) with platonic shapes,³⁴ through a one-pot polyol/PVP process (Fig. 6f). The ratio of gold salt to PVP appeared to be an important parameter; tetrahedra formed at higher gold/PVP ratios and icosahedra at lower ratios. However, the presence of small amounts of silver ions (~1% of the gold precursor) induced formation of uniform gold nanocubes. Other authors explored the influence of various additives such as citric acid, Fe(III), or NaOH, in line with the oxidative etching mechanism proposed by Xia’s group for shape control in silver particles.³⁵

An interesting contribution to shape control in polyhedral particles was provided by Seo *et al.*, who refluxed metal salts in 1,5-pentanediol–PVP solutions. Again, addition of silver nitrate was used to tune the particle shape with no need for seeds.³⁶ In a key experiment, starting from cuboctahedral particles, overgrowth in the absence of silver nitrate yielded large octahedra, while in the presence of silver nitrate large cubes were formed from the same seeds (see Fig. 6e). Therefore, octahedra, truncated octahedra, cuboctahedra and cubic particles could be easily interconverted using seeded growth in the presence or absence of silver nitrate, which seems once more to be related again to selective blocking of certain crystallographic facets.

The influence of the crystalline structure of the seed was studied by Liz-Marzán and co-workers, who developed a seeded-growth method based on ultrasound-induced reduction of a gold salt in DMF–PVP solution.³⁷ It was found that when pre-formed penta-twinned gold nanoparticle seeds were used, regular and nearly monodisperse decahedra were formed (Fig. 6a), while growth on single-crystalline platinum seeds yielded perfect, single crystal octahedra (Fig. 6b). The dimensions of both types of particle could be easily controlled by varying the relative concentrations of seed particles and gold salts. In a related experiment, Carbó-Argibay *et al.* used gold nanorods prepared in water as seeds for growth in DMF–PVP solution.³⁸ This led to complete reshaping of the rods through

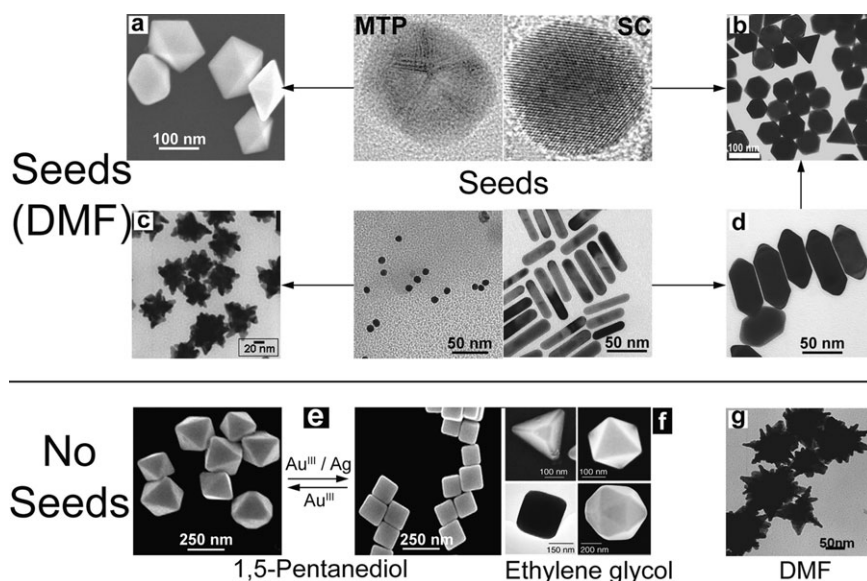


Fig. 6 Electron micrographs of Au nanoparticles with various shapes, synthesised through DMF/polyol reduction in the presence of PVP. In the upper panel, seeded growth is summarised, while the particles shown in the lower panel were made with no pre-made seeds.

tip sharpening (Fig. 6d), faceting of the lateral faces, and ultimately led to perfect, single-crystalline octahedra.

Finally, the non-aqueous synthesis of nanoplates and branched structures is still in its infancy. While the formation of silver plates is rather well established, nanometre sized gold plates have been reported only in rather low yields. Branched “nanostars” were recently reported³⁹ through room temperature growth, in a concentrated solution of PVP in DMF. Although size control was demonstrated when 15 nm seeds were present (Fig. 6c), stars were also obtained in a similar seedless process (Fig. 6g), and much work is still needed to achieve true morphology control. The beauty of these particles is that each tip is a single crystal, so the challenge remains to understand the underlying growth mechanism from a central seed. However at this point we can still summarise the main effects that appear to be responsible for shape control in the non-aqueous polyol method:

- The adsorption of PVP molecules to the particular crystal facets has been invoked by several authors as the key parameter determining the particle shape and crystalline structure.^{34,38}

- The selective underpotential deposition of silver ions onto {100} gold surfaces may suppress the epitaxial overgrowth of additional gold layers, thus governing the final shape through selective surface overgrowth.³⁶

- The crystalline structure of the seeds definitely influences the growth, the important issue being whether the seed particles are twinned or single crystalline structures.³⁷

- The addition of small amounts of different salts can strongly influence the final particle shape through selective adsorption on certain gold facets or changes in their relative surface energy.

5. Conclusions and perspectives

The initial report on the growth of gold rods by Wang *et al.*¹³ through electrochemical reduction in the presence of cationic

surfactants has sparked an enormous amount of work on shape control. The number and type of efficacious shape-controlling additives identified thus far remains very limited, which suggests that chemical interactions are important. For anisotropic growth of gold and silver nanoparticles, the interplay of halide ions is critical, and a general mechanism based on simple facet blocking does not explain many features of anisotropic particle growth.

Although a large variety of geometries have also been produced through reduction of metal salts in organic solvents, the fundamental parameters involved have not been clearly discerned, and there is still much room for improvement before rational nanoparticle design is achieved.

The theme of this tutorial review has been the emergence of shape control of metal particles. While we have examined the chemical mechanisms that lead to anisotropic particle growth, much of this interest in the case of metal particles has been stimulated by the fact this leads to a mechanism to tune the surface plasmon resonances of such particles (see review by Myroshnychenko *et al.*⁴⁰ within this issue). However, in the longer term the greater impact may well be in providing a proper basis for the way materials in general are engineered. The most obvious of these directions will be in biomimetic materials. Note that it is not necessary to grow whole bones or teeth *ex situ*, as is sometimes envisaged. More likely, anisotropic crystals together with guide proteins and biocompatible coatings will be inserted as nuclei and allowed to grow “naturally” into engineered shapes and morphologies, somewhat like stem cells. As shape control improves there will be an increasing need for mechanical studies of the crystals to establish which morphologies offer the highest toughness, Young’s modulus, elasticity, shape memory, crack resistance and corrosion inhibition. Another field where anisotropic crystals may become important is in printed electronics. Printing anisotropic shapes by ink-jet printing colloid particles is limited in terms of architecture. One may imagine that metal

nanoprisms printed appropriately to form a mosaic and then annealed will form flat, conducting channels, superior to aggregated spheres and with lower sheet resistance. Conversely, needles deposited vertically could provide interconnects, while nanostars may form supercapacitors by maintaining high surface area within a conducting structure. What is clear from such perspectives is that once shape control of crystals is achieved, assembly into useful functional architectures will remain an important challenge.

Acknowledgements

This work was supported by the Spanish MEC (MAT2007-62696) and Xunta de Galicia. PM acknowledges support through an ARC Federation Fellowship FF0561486 and DP Grant 0451651.

References

- 1 S. Eustis and M. A. El-Sayed, *Chem. Soc. Rev.*, 2006, **35**, 209.
- 2 C. Burda, X. Chen, R. Narayanan and M. A. El-Sayed, *Chem. Rev.*, 2005, **105**, 1025.
- 3 L. M. Liz-Marzán, *Langmuir*, 2006, **22**, 32.
- 4 J. Pérez-Juste, I. Pastoriza-Santos, L. M. Liz-Marzán and P. Mulvaney, *Coord. Chem. Rev.*, 2005, **249**, 1870.
- 5 M.-D. Daniel and D. Astruc, *Chem. Rev.*, 2004, **104**, 293.
- 6 C. Lofton and W. Sigmund, *Adv. Funct. Mater.*, 2005, **15**, 1197.
- 7 N. R. Jana, L. Gearheart and C. J. Murphy, *Adv. Mater.*, 2001, **13**, 1389.
- 8 B. Nikoobakht and M. A. El-Sayed, *Chem. Mater.*, 2003, **15**, 1957.
- 9 C. J. Johnson, E. Dujardin, S. A. Davis, C. J. Murphy and S. Mann, *J. Mater. Chem.*, 2002, **12**, 1765.
- 10 M. Liu and P. Guyot-Sionnest, *J. Phys. Chem. B*, 2005, **109**, 22192.
- 11 N. R. Jana, L. Gearheart and C. J. Murphy, *J. Phys. Chem. B*, 2001, **105**, 4065.
- 12 J. Pérez-Juste, L. M. Liz-Marzán, S. Carnie, D. Y. C. Chan and P. Mulvaney, *Adv. Funct. Mater.*, 2004, **14**, 571.
- 13 Y.-Y. Yu, S.-S. Chang, C.-L. Lee and C. R. C. Wang, *J. Phys. Chem. B*, 1997, **101**, 6661.
- 14 T. K. Sau and C. J. Murphy, *J. Am. Chem. Soc.*, 2004, **126**, 8648.
- 15 X. Kou, S. Zhang, Z. Yang, C.-K. Tsung, G. D. Stucky, L. Sun, J. Wang and C. Yan, *J. Am. Chem. Soc.*, 2007, **129**, 6402.
- 16 J. E. Millstone, S. Park, K. L. Shuford, L. Qin, G. C. Schatz and C. A. Mirkin, *J. Am. Chem. Soc.*, 2005, **127**, 5312.
- 17 B. D. Busbee, S. O. Obare and C. J. Murphy, *Adv. Mater.*, 2003, **15**, 414.
- 18 T. H. Ha, H.-J. Koo and B. H. Chung, *J. Phys. Chem. C*, 2007, **111**, 1123.
- 19 C. S. Ah, Y. J. Yun, H. J. Park, W.-J. Kim, D. H. Ha and W. S. Yun, *Chem. Mater.*, 2005, **17**, 5558.
- 20 S. S. Shankar, A. Rai, B. Ankamwar, A. Singh, A. Ahmad and M. Sastry, *Nat. Mater.*, 2004, **3**, 482.
- 21 S. S. Shankar, A. Rai, A. Ahmad and M. Sastry, *Chem. Mater.*, 2005, **17**, 566.
- 22 J. Xie, J. Y. Lee and D. Y. C. Wang, *J. Phys. Chem. C*, 2007, **111**, 10226.
- 23 S. Chen, Z. L. Wang, J. Ballato, S. H. Foulger and D. L. Carroll, *J. Am. Chem. Soc.*, 2003, **125**, 16186.
- 24 C. L. Johnson, E. Snoeck, M. Ezcurdia, B. Rodríguez-González, I. Pastoriza-Santos, L. M. Liz-Marzán and M. J. Hÿtch, *Nat. Mater.*, 2008, **7**, 120.
- 25 J. Gao, C. M. Bender and C. J. Murphy, *Langmuir*, 2003, **19**, 9065.
- 26 L. B. Rogers, D. P. Krause, J. C. Griess and D. B. Ehrlinger, *J. Electrochem. Soc.*, 1949, **95**, 33.
- 27 D. M. Kolb, M. Przasnyski and H. Gerischer, *J. Electroanal. Chem. Interfacial Electrochem.*, 1974, **54**, 25.
- 28 H. B. Michaelson, *IBM J. Res. Dev.*, 1978, **22**, 72.
- 29 P. Mulvaney, *Langmuir*, 1996, **12**, 788.
- 30 J. Hernández, J. Solla-Gullón, E. Herrero, A. Aldaz and J. M. Feliu, *J. Phys. Chem. B*, 2005, **109**, 12651.
- 31 R. Michalitsch, B. J. Palmer and P. E. Laibinis, *Langmuir*, 2000, **16**, 6533.
- 32 C. Chun-hsien, S. M. Vesceky and A. A. Gewirth, *J. Am. Chem. Soc.*, 1992, **114**, 451.
- 33 C. J. Orendorff and C. J. Murphy, *J. Phys. Chem. B*, 2006, **110**, 3990.
- 34 F. Kim, S. Connor, H. Song, T. Kuykendall and P. Yang, *Angew. Chem., Int. Ed.*, 2004, **43**, 3677.
- 35 B. Wiley, Y. Sun, B. Mayers and Y. Xia, *Chem.–Eur. J.*, 2005, **11**, 454.
- 36 D. Seo, C. I. Yoo, J. C. Park, S. M. Park, S. Ryu and H. Song, *Angew. Chem., Int. Ed.*, 2008, **47**, 763.
- 37 A. Sánchez-Iglesias, I. Pastoriza-Santos, J. Pérez-Juste, B. Rodríguez-González, F. J. García de Abajo and L. M. Liz-Marzán, *Adv. Mater.*, 2006, **18**, 2529.
- 38 E. Carbó-Argibay, B. Rodríguez-González, J. Pacifico, I. Pastoriza-Santos, J. Pérez-Juste and L. M. Liz-Marzán, *Angew. Chem., Int. Ed.*, 2007, **46**, 8983.
- 39 P. S. Kumar, I. Pastoriza-Santos, B. Rodríguez-González, F. J. García de Abajo and L. M. Liz-Marzán, *Nanotechnology*, 2008, **19**, 015606.
- 40 V. Myroshnychenko, J. Rodríguez-Fernández, I. Pastoriza-Santos, A. M. Funston, C. Novo, P. Mulvaney, L. M. Liz-Marzán and F. J. García de Abajo, *Chem. Soc. Rev.*, 2008, DOI: 10.1039/b711486a.